Journal of Engineering Science and Technology
Vol. 16, No. 3 (2021) 1932 - 1950

GREY-WOLF OPTIMIZATION BETTER ENHANCES THE DYNAMIC PERFORMANCE OF ROLL MOTION FOR TAIL-SITTER VTOL AIRCRAFT GUIDED AND CONTROLLED BY STSMC

ARIF A. AL-QASSAR[1,*], AHMED I. ABDULKAREEM[1], ALAQ F. HASAN[2], AMJAD J. HUMAIDI[1], IBRAHEEM KASIM IBRAHEEM[3], AHMAD TAHER AZAR[4,5], AKRAM H. HAMEED[6]

[1]Control and Systems Engineering Department, University of Technology, Baghdad, Iraq
[2]Technical Engineering College, Middle Technical University, Baghdad, Iraq
[3]University of Baghdad, College of Engineering, Electrical Engineering Dept., Iraq
[4]Prince Sultan University, Riyadh, Kingdom of Saudi Arabia
[5]Faculty of Computers and Artificial Intelligence, Benha University, Egypt
[6]Ministry of Electricity, Baghdad State Co. of Elect. Distribution, Iraq, Baghdad
*Corresponding Author: 60023@uotechnology.edu.iq

Abstract

This article presents the design of optimal sliding mode control (SMC) and optimal super-twisting sliding mode control (STSMC) for the roll motion of vertical take-off and landing (VTOL) unmanned air vehicle (UAV) in hovering flight under nonparametric uncertainty (gust and wind disturbance). The stability analysis of the controlled roll motion has been presented and asymptotic error convergence has been proven based on Lyapunov theorem. Accordingly, the control laws are developed for the aircraft system subjected to uncertainty. To avoid the try-and-error procedure in the selection of the design parameters and to improve the performances of SMC and STSMC, the grey-wolf optimization has been suggested for tuning purposes. Based on numerical simulation, a comparison study has been conducted between the optimal and non-optimal controllers, and also between optimal SMSTC and optimal SMC in terms of tracking error and chattering behaviour in control signals. The numerical simulation showed that the GWO could enhance the performances of SMC and STSMC. Also, the optimal STSMC has better dynamic performance than the optimal SMC in terms of tracking error and chattering effect in control signal.

Keywords: Grey-wolf optimization, Guidance, Roll motion, Stability analysis, Super-twisting sliding mode control, Tail-sitter VTOL aircraft.

1. Introduction

In the last years, the Unmanned Aerial Vehicles (UAVs) have acquired fast-growing popularity world-wide and experienced enormous development. Nowadays, these UAVs are largely applied in different critical military and defence purposes like reconnaissance, security reinforcement, and surveillance. However, in addition of military and defence applications of UAVs, the usage of these small aircraft has rapidly grown in many military and civilian applications, and they have incorporated in wide range of fields including disaster management, vegetarian monitoring, traffic surveillance, infrastructure inspection, and law enforcement [1].

There are other missions of UAV which extend the scope of conventional capabilities of small UAVs. The longer endurance of flight is not only the requirement of most missions, but also the vertical take-off and landing (VTOL) and hovering capabilities. Moreover, the capability of conversion from one configuration to another is the other required task of these small aircrafts, which became necessary demand recently. Combing the forward flight characteristics of fixed-wing aircraft with the take-off and landing capabilities of the helicopter will result in promising UAVs which characterized by unique flexible operation capabilities at low cost than other conventional UAVs [2].

The tail-sitter vehicle is one configuration of these convertible aircrafts. It is characterized by taking the vertical airframe attitude during landing and take-off, while takes the attitude of horizontal airframe in case of cruising just like conventional airplanes. However, the flight dynamics of tail-sitters are characterized by high complexity, particularly in hover mode, which makes them very difficult to control [2]. In what follows, some of the relevant and recent control strategies used for flight control of tail-sitter aircraft are briefly discussed.

In Barth et al. [3] applied model-free control scheme for stabilization of tail-sitter micro-aircraft attitude in the presence of wind disturbance. Four flight modes have been taken into account; particularly, vertical take-off, transitioning flight, forward flight, hovering and vertical landing. In Zhou et al. [4], established flight control design based on model predictive control (MPC) and successive linearization for VTOL tail-sitter aircraft in the hovering mode. In Wang et al. [5], presented a novel control design for tail-sitter aircraft actuated by twin rotors. The proposed control configuration is based on decreasing the distance between rotors and elevators, which results in maximizing the speed flow and in turn lead to generating the required control torque necessary to stabilizing the twin-rotor aircraft against disturbing wind.

Garcia-Nieto et al. [6] have presented the design of attitude tracking controller for unmanned flying-wing actuated by two tilting rotors to achieve VTOL manoeuvre in hovering operation. The efficiency of proposed controller has been tested based on both Hardware-In-the-Loop (HIL) simulation test and experimental test. Ge and Hou [7] have combined the design of fuzzy self-tuning PID control and L1- adaptive control for stabilization of longitudinal attitude of tail-sitter aircraft subjected to uncertainties. This study has applied the algorithm of double-Euler angle method in modelling to solve the singularity problem due to fuselage tilting. Abrougui et al. [8] has designed and developed a flight regulation control algorithm based on PID (Proportional, Integral and Derivative) controller for stabilization of roll motion for the VTOL aircraft during the operation of hovering

flight. In Flores et al. [9], has presented a control design based on linear saturation functions and Lyapunov approach for manoeuvre in transition for tail-sitter drone.

In Garcia et al. [10] developed a control algorithm based on separated saturation functions to stabilize the attitude of single-rotor actuated tail UAV affected by perturbation in the channel of vertical take-off and landing operation. Verling et al. [11] have proposed both structure design and control design of convertible VTOL tail-sitter aircraft. The development of UAV has combined the merits of technologies in both rotary and fixed wing UAV systems. A unified controller has been synthesized and designed to address the aircraft dynamics at any configuration and attitude like rotor-actuated scheme, fixed-wing scheme, or the transition from one configuration to another. This unified controller can achieve monotonic transition in switching from one mode to another without any discontinuity. Li et al. [12] presented the design of control algorithm based on MPC (Model Predictive Control) for motion control of tail-sitter VTOL aircraft during hovering flight operation. The control design of MPC is based on augmentation of linearized model. The disturbance rejection capability has been improved using an optimization technique. Çakici and Leblebicioğlu [13] have proposed the control design for stabilization of fixed-wing and multi-rotors actuated aircraft. Three modes of flight have been considered for the suggested UAV: Vertical-Take-off-Landing (VTOL), hovering and level flight mode. The control algorithm has been developed to switch between the modes of flight.

Like most aircrafts, the dynamics of tail-sitters encounter dramatic variations during their flight and the need of robust controller is a pre-requisition to solve this challenging problem. However, the use of conventional controller is awesome for these kinds of aerial systems. One of the drawbacks of conventional tracking controllers is that they are unable to cope with unknown load characteristics over a widely ranging of operating point. This study adopts the super-twisting sliding mode control (STSMC) design to cope with the uncertainty due to the gust wind in roll motion of the considered aircraft.

The STSMC is one new type of sliding mode control (SMC), which features with by the following merits [14-20].

- In case of STSMC, the chattering effect in control signal is less than SMC.
- The STSMC design has the ability to make the trajectories of system solution to reach the equilibrium states in finite time. In other words, the zeroing of both state and its derivative in finite time is possible with STSMC.
- In STSMC, there is need for the derivative of states, but only for the sliding variable or output variable. Therefore, STSMC differs from most SMC techniques in that the knowledge of state derivatives is not required. This in turn will lead to simple synthesized control law and to less effort of computation.
- Exact convergence and singularity avoidance can be achieved with STSMC.

According to the above features, the STSMC has been adopted to control the roll motion of VTOL aircraft.

A critical issue in control design of STSMC is how to set the values of design parameters arising throughout the stability analysis of the controlled system for developing the required control law. These design parameters play a vital role in performance of STSMC. Frequently, their setting is based on the try-and-error

procedure. This procedure is old, and it lacks the ability to find the optimal performance of STSMC. Recently, modern optimization techniques are incorporated for tuning these parameters such as to improve the dynamic response of the system controlled by STSMC in terms of minimum tracking error. In this study, the Grey Wolf Optimization algorithm (GWO) has been proposed to adjust the design parameters of STSMC. The GWO is a new meta-heuristic optimization algorithm proposed in 2014 [21]. It has been widely used in different applications due to its excellent performance [22, 23]. The contribution of this study can be summarized in the following points:

- Design of roll motion control for the tail-sitter VTOL aircraft based on STSMC.
- Design an optimization algorithm based on GWO technique to improve the performance of STSMC and SMC by tuning their design parameters and to replace the try-and-error procedure.
- Conducting a comparative study between optimal and non-optimal versions of SMC and STSMC. Also, a comparison study is made between optimal SMC and optimal STSMC for the tail-sitter VTOL aircraft system via numerical simulation.

2. The Dynamic Model of Tail-Sitter VTOL Aircraft

This part considers the development of dynamic model for the tail-sitter VTOL aircraft. Firstly, two assumptions are made to proceed in deriving the dynamic model:

Assumption 1: The aircraft operates within small local region. This will justify applying the model equation of flat earth [13].

Assumption 2: The masses of blade and elevators have been neglected [24].

Referring to Fig. 1, let the coordinate system (X, Y, Z) represents the body fixed frame $(b - frame)$ and the north-east-down (NED) coordinate system (x, y, z) represents the inertial reference frame $(n - frame)$. Based on Fig. 1, the kinematic equations describing the position, the forces and the moments are represented by [25]:

$$\dot{p} = R(e)\, V \tag{1}$$

$$\dot{\Theta} = H(e)\, \Omega \tag{2}$$

$$m\, \dot{V} = -\Omega \times V + F \tag{3}$$

$$J\, \dot{\Omega} = -\Omega \times J.\, \Omega + \tau \tag{4}$$

where $p = [p_n \;\; p_e \;\; p_d]^T$ represents the positions of mass centre of rigid body relative to the $(n - frame)$, $e = [e_o \;\; e_1 \;\; e_2 \;\; e_3]^T$ represent the quaternion of the current attitude and it is defined by $e = e_o + e_1 i + e_2 j + e_3 k$, $\Theta = [\phi \;\; \theta \;\; \psi]^T$ represents the orientation of the VTOL aircraft in the $(n - frame)$, where the Euler angles ϕ, θ and ψ defines the roll, pitch and yaw angles, which are commonly used in aerodynamic applications. The vector $\Omega = [P \;\; Q \;\; R]^T$ represents the angular velocity in the body fixed frame $(b - frame)$, F is the vector of external thrusts applied to mass center of the VTOL aircraft, the torque vector $\tau = [\tau_l \;\; \tau_m \;\; \tau_n]^T$ combines the torque components exerted to the centre of VTOL aircraft mass in the body frame and J is the inertia matrix of the flying aircraft, which is given by

$$J = \begin{bmatrix} J_x & J_{xy} & J_{xz} \\ J_{yx} & J_y & J_{yz} \\ J_{zx} & J_{zy} & J_z \end{bmatrix} \tag{5}$$

If it is assumed the body axis xz-plane of the configuration of tail-sitter VTOL aircraft is coincident with the plane of symmetry, then the products of inertia J_{xy} and J_{yz} vanishes. Also, the tail-sitter configuration has a plane of symmetry in the yz-plane, this leads that the product of inertia J_{xz} equal to zero. Then the inertia matrix and its inverse become

$$J = \begin{bmatrix} J_x & 0 & 0 \\ 0 & J_y & 0 \\ 0 & 0 & J_z \end{bmatrix}, J^{-1} = \begin{bmatrix} 1/J_x & 0 & 0 \\ 0 & 1/J_y & 0 \\ 0 & 0 & 1/J_z \end{bmatrix} \tag{6}$$

The transformation matrix H given in Eq. (2), transforms the components of the angular velocity, generated by Euler rotations, from the body frame to the inertial frame is given by:

$$H(e) = \begin{bmatrix} 1 & \tan(\theta)\ \sin(\phi) & \tan(\theta)\ \cos(\phi) \\ 0 & \cos(\phi) & -\sin(\phi) \\ 0 & \sin(\phi)/\cos(\theta) & \cos(\phi)/\cos(\theta) \end{bmatrix} \tag{7}$$

Therefore, the kinematic Eq. (2) can be written as follows:

$$\dot{\phi} = P + \tan\theta\,(Q\sin(\theta) + R\cos\phi) \tag{8}$$

$$\dot{\theta} = Q\cos\phi - R\sin\phi \tag{9}$$

$$\dot{\psi} = (Q\sin\phi + R\cos\phi)/\cos\theta \tag{10}$$

Using the inertia matrix given by Eq. (6) and using the thrust moments T_l, T_m and T_n as indicated in Fig. 1, Eq. (4) can be rewritten by:

$$\dot{P} = (J_y - J_z)\,QR/J_x + T_l/J_x \tag{11}$$

$$\dot{Q} = (J_z - J_x)\,PR/J_y + T_m/J_y \tag{12}$$

$$\dot{R} = (J_x - J_y)\,PQ/J_z + T_n/J_z \tag{13}$$

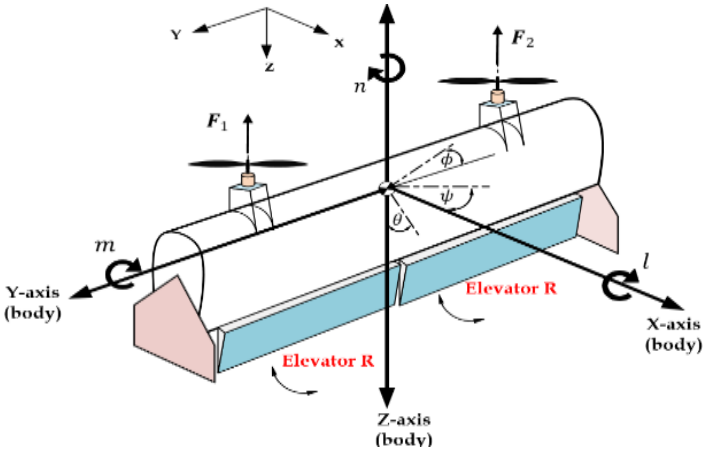

Fig. 1. Flight dynamics of tail-sitter VTOL aircraft [25].

In order to extract the roll dynamic, it is assumed that the yaw and pitch rates are set to zero; that is, $P = Q = 0$. Based on this assumption, the configuration of tail-sitter VTOL aircraft can be shown in Fig. 2. Therefore, based on Eqs. (6) and (9), the rotational dynamics can be represented for the roll angle using the following simple dynamic equation:

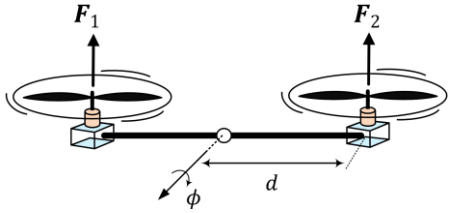

Fig. 2. The configuration of roll dynamics.

$$\ddot{\phi} = T_l / J_x \tag{14}$$

where the exerted torque T_l can be calculated as follows:

$$T_l = F.d - C_l\,\dot{\phi} \tag{15}$$

where $F = F_1 - F_2$ represents the resultant force between the force due to right rotor and left rotor, d is the distance between the mass center and reach rotor. The term $C_l\,\dot{\phi}$ is the drag force, which represents the aerodynamic moment that works to oppose the rolling moment with damping coefficient of C_l.

Combining Eq. (14) and Eq. (15) and taking into account the effect of gust wind as uncertainty $\zeta(t)$ applied to the roll dynamic system to have,

$$\ddot{\phi} = (-C_l\,\dot{\phi} + F.d)/J_x + \zeta(t) \tag{16}$$

Equation (16) can be rewritten as

$$\ddot{\phi} = f_o + b\,u + \zeta(t) \tag{17}$$

where f_o , b and u are represented by $f_o = -C_l\,\dot{\phi}/J_x$; $b = d/J_x$; $u = F$.

Remark *1*: $\zeta(t)$ is the gust wind, the derivative of uncertainty satisfies $|\dot{\zeta}(t)| \leq \gamma$, where γ is the upper bound of the derivative of the uncertainties, which is a positive constant.

3. Super Twisting Sliding Mode Control for Tail-Sitter VTOL Aircraft

Let e defines the tracking error between the actual roll angle (ϕ) and the desired roll angle (ϕ_d),

$$e = \phi - \phi_d \tag{18}$$

The time derivative of error is given by

$$\dot{e} = \dot{\phi} - \dot{\phi}_d \tag{19}$$

The sliding surface can be defined by

$$s = \dot{e} + \lambda\,e \tag{20}$$

Taking the time derivative of Eq. (20), one can have

$$\dot{s} = \ddot{e} + \lambda\dot{e} = \ddot{\phi} - \ddot{\phi}_d + \lambda\dot{e} \quad \text{or } \dot{s} = f_o + \zeta(t) + b\,u - \ddot{\phi}_d + \lambda\dot{e} \tag{21}$$

In the sense of sliding control theory, the control law is composed of two parts: equivalent part and switching part; that is,

$$u = \frac{1}{b}\left(u_{eq} + u_{sw}\right) \tag{22}$$

By setting $s = \dot{s} = 0$, one can easily obtain the equivalent part of control law. Accordingly, based on Eq. (21), the equivalent component can be found

$$u_{eq} = -f_o + \ddot{\phi}_d - \lambda\dot{e} \tag{23}$$

The switch part is proposed, based on STSMC, to be

$$u_{sw} = -c_1\sqrt{|s|}\,sgn(s) - c_2\int sgn(s)\,dt \tag{24}$$

Therefore, the control law can now be determined as follows

$$u = \frac{1}{b}\left(-f_o + \ddot{\phi}_d - \lambda\dot{e} - c_1\sqrt{|s|}\,sgn(s) - c_2\int sgn(s)\,dt\right) \tag{25}$$

Accordingly, Eq. (21) becomes

$$\dot{s} = -c_1\sqrt{|s|}\,sgn(s) - c_2\int sgn(s)\,dt + \zeta(t) \tag{26}$$

The asymptotic stability of the tail-sitter VTOL aircraft, controlled by super-twisting SMC, can be assured by choosing the following Lyapunov function is chosen,

$$V = \frac{1}{2}.s^2 \tag{27}$$

Combining the time derivative of Eq. (27) with Eq. (26) to have

$$\dot{V} = s\left(-c_1\sqrt{|s|}\,sgn(s) - c_2\int sgn(s)\,dt + \zeta(t)\right) \tag{28}$$

Based on the elementary linear algebra and the mathematical fact $s.sgn(s) = |s|$, Eq. (28) can be expressed by

$$\dot{V} \le -c_1\sqrt{|s|}\,|s| - |s|\int c_2\,dt + |\zeta(t)\,s|$$

$$\dot{V} \le -c_1\sqrt{|s|}\,|s| - |s|\int c_2\,dt + |s|\int\left|\dot{\zeta}(t)\right|dt$$

As we assume in remark 1 that $\left|\dot{\zeta}(t)\right| \le \delta$, where δ is a positive constant and it represents the upper bound of the derivative of the uncertainty, then the previous equation can be written as

$$\dot{V} \le -c_1\sqrt{|s|}\,|s| - |s|\int c_2\,dt + |s|\int \gamma\,dt$$

$$\dot{V} \le -c_1\sqrt{|s|}\,|s| - |s|(\int c_2\,dt - \int \gamma\,dt) \tag{29}$$

Remark 2**:** The stability of tail-sitter VTOL aircraft, controlled by STSMC, can be guaranteed if the value of c_2 satisfies $c_2 > \gamma > \left|\dot{\zeta}(t)\right|$.

The schematic diagram of roll motion-controlled VTOL aircraft based on is indicated in Fig. 3.

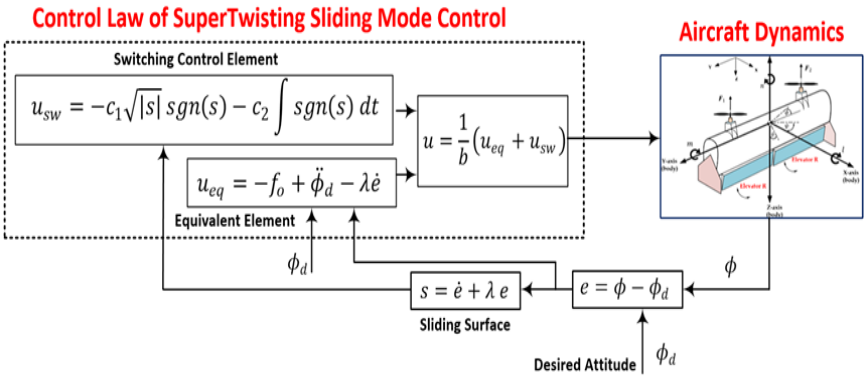

Fig. 3. Schematic diagram of super-twisting sliding mode attitude-controlled VTOL aircraft.

Other control strategies can be suggested to extend this study for future work. The active disturbance rejection control, observer-based control, backstepping control, adaptive control, RISE control, nonlinear PD control, model predictive control, and extremum seeking control can be included for roll stabilization and control of tail-sitter VTOL such that a comparison study in performance can be conducted between the proposed controller and one of these control schemes [26-38].

4. Classical Sliding Mode Control for Tail-Sitter VTOL Aircraft

The switch part in the classical SMC is proposed as [39, 40],

$$u_{sw} = k\ sgn(s) \tag{30}$$

Therefore, one can write the control law as follows:

$$u = \frac{1}{b}\left(-f_o + \ddot{\phi}_d - \lambda_1\dot{e} - k\ sgn(s)\right) \tag{31}$$

Accordingly, Eq. (21) becomes

$$\dot{s} = -k\ sgn(s) + \zeta(t) \tag{32}$$

To establish the stability analysis of VTOL aircraft based on classical SMC, one can choose a Lypunov function of the following form,

$$V = \frac{1}{2}s^2 \tag{33}$$

Again, taking the time derivative of Eq. (33) and applying Eq. (32) to have

$$\dot{V} = s\left(-k\ sgn(s) + \zeta(t)\right) \tag{34}$$

Based on the elementary linear algebra and the mathematical fact $s.sgn(s) = |s|$, Eq. (34) can be expressed by

$$\dot{V} \leq -k\,|s| + |\zeta(t)\,s|\ ; \dot{V} \leq -k\,|s| + |s|\int\left|\dot{\zeta}(t)\right|dt\ ;$$

$$\dot{V} \leq |s|\left(-k\ + \int\left|\dot{\zeta}(t)\right|dt\right) \tag{35}$$

Remark 3: The stability of the tail-sitter VTOL aircraft, controlled by SMC, is guaranteed if the value of k satisfies $k > \int \gamma\ dt$.

5. GWO-Based STSMC

In this part, GWO algorithm is used to find the optimal values of these parameters in terms of better performance of tacking based on STSMC of tail-sitter VTOL aircraft [40-44].

5.1. Social hierarchy

Grey wolves are social animals, and they have a strict social hierarchy. The population is divided into four levels, namely α, β, δ and ω. Corresponding to the GWO algorithm, we denote the individual with the highest fitness as α. The two suboptimal individuals are β and δ. ω represents the remaining individuals. The optimization process of GWO is mainly guided by the three individuals with the best fitness in the population.

5.2. Encircling prey

The grey wolf usually approaches and surrounds the prey gradually, and the process of grey wolves surrounding their prey can be presented as

$$D = |C.X_P(t) - X(t)| \tag{36}$$

where t is the current iteration, X_P is the location of the prey, X is the position of the grey wolf, and $C = 2.r_1$ and $r_1 \in [0,1]$ is a random number.

$$X(t+1) = X_P(t) - A.D \tag{37}$$

where $A = 2ar_2$-a, a gradually decrease from 2 to 0, $r_2 \in [0,1]$ is a random number.

5.3. Hunting

Assume that namely α, β and δ can track the prey effectively. At every iteration, the positions of the other grey wolves are updated based on the position information of wolves α, β and δ. The mechanism of wolf position updating is shown in Fig. 4. In Fig. 4, D_α, D_β and D_δ are the distance between wolves ω and wolves α, β and δ which have the best fitness.

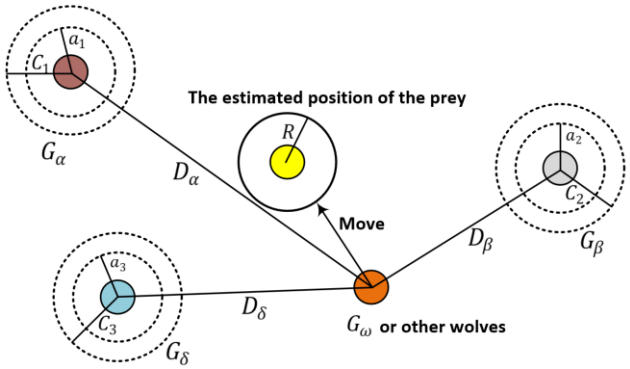

Fig. 4. Wolf hunting mechanism [41].

The mathematical description of the hunting process is

$$D_\alpha = |C_1.X_\alpha - X|$$

$$
\begin{aligned}
D_\beta &= \left|C_2 . X_\beta - X\right| \\
D_\delta &= \left|C_3 . X_\delta - X\right| \\
X_1 &= X_\alpha - A_1 . D_\alpha \\
X_2 &= X_\beta - A_2 . D_\beta \\
X_3 &= X_\delta - A_3 . D_\delta \\
X(t+1) &= \frac{X_1 + X_2 + X_3}{3}
\end{aligned} \tag{38}
$$

where X_α, X_β and X_δ are the positions of α, β and δ, respectively. C_1, C_2 and C_3 are three random vectors, and X is the current location of the grey wolf. The list of algorithm steps for grey-wolf optimization is given below:

Optimization algorithm of grey-wolf technique

Initialize the grey wolf population X_i $(i = 1,2, \ldots\ldots, n)$
Initialization of a, A, and C
Calculation of fitness for each search agent
Set X_α for the best search agent
Set X_β for the second-best search agent
Set X_δ for the third best search agent
While (stopping criteria has not been reached) do
    for each search agent
        Update the position of the current search agent using Eq. (38)
    end for
    Update the parameters: a, A, and C
    Calculation of the fitness for all search agents
    Update the variables X_α, X_β, and X_δ
    t=t+1
end while
Output the best solution found

Other optimization techniques like cuckoo optimization algorithm, sine-cosine algorithm, whale optimization, spider social optimization, and monkey-spider optimization can be suggested to tune the design parameters of both SMC and STSMC and to establish a comparison study in performance with grey-wolf optimization [41-51].

6. Computer Simulation

In this section, the effectiveness of STSMC and SMC have been evaluated via numerical simulation using MATLAB programming software. The numerical simulation has used Ode45 as a numerical solver. Table 1 gives the numerical values of parameters for the considered tail-sitter VTOL aircraft.

Table 1. Numeric parameters of tail-sitter VTOL aircraft.

Parameter	Description	Value
J_x	x-axis moment of inertia	0.0144 kg. m^2
C_L	Roll damping coefficient	0.36
d	The rotor distance from mas center	0.2 m

The optimization algorithm based on GWO results in optimal design parameters for STSMC and SMC and hence an optimal STMSC and optimal SMC will be obtained. Table 2 lists the values of optimal design parameters given by GWO. The simulation results have been initiated by showing the behaviors of cost functions w.r.t the optimization iterations, as illustrated in Fig. 5.

Table 2. The optimal setting of design parameters based on GWO algorithm.

Design Parameters		Value
SMC	λ_1	3
	k	3
STSMC	c_1	2.5
	c_2	2
	λ	3

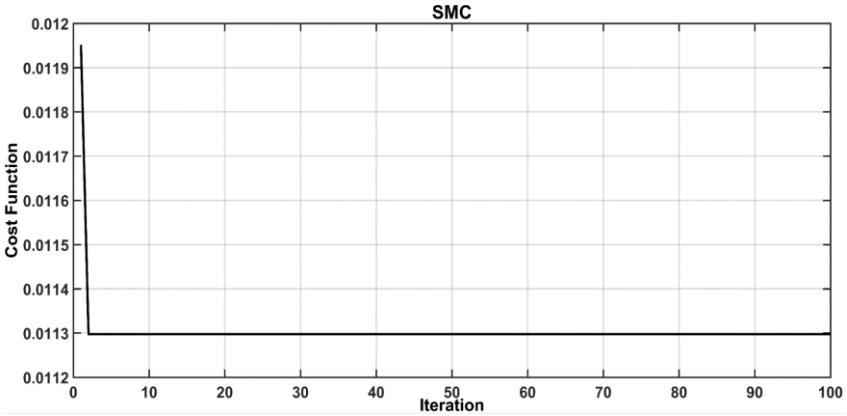

(a) STSMC.

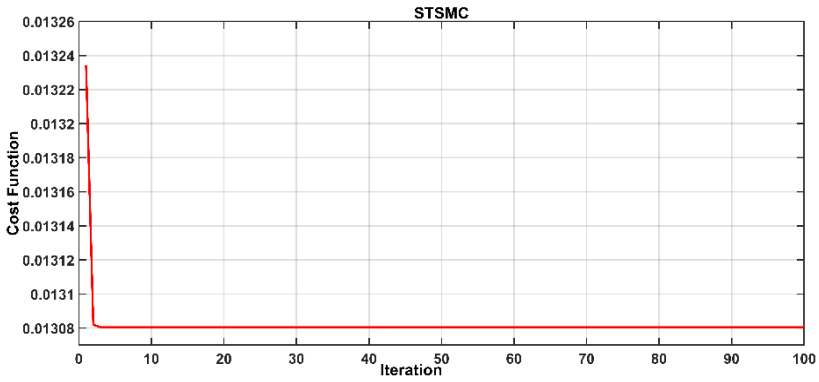

(b) SMC.

Fig. 5. Evolution of the cost function versus the iterations.

In the present wok, two scenarios have been presented. The first scenario presents the uncertainty-free case, while the uncertainty has been accounted for in the second

scenario. The tracking behaviors of the roll angle for VTOL aircraft system in the uncertainty-free case system are shown in Fig. 6, based on optimal and non-optimal SMCs. On the other hand, Fig. 7 shows the tracking behaviour of the roll angle based on optimal and non-optimal STSMC. The behaviour error (e) for all designed controllers are shown in Figs. 8 and 9, where e represents the difference between the desired signal and the output. Table 3 shows the tracking performance of tail-sitter VTOL aircraft based on the controllers. Figure 10 shows the behaviour of control law under this situation. Based on Table 3, one can deduce that the optimal STSMC has better performance than the optimal SMC. In addition, the chattering shown in control signal in case of STSMC is lower than that based on SMC.

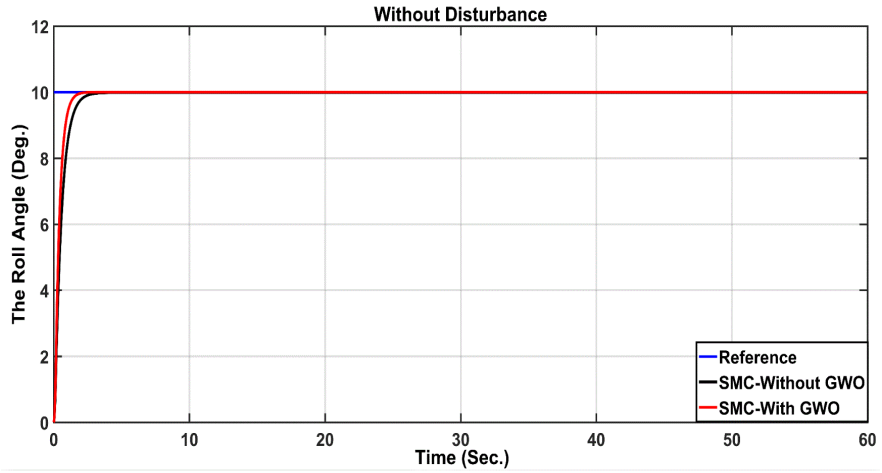

Fig. 6. Behavior of roll angle SMC.

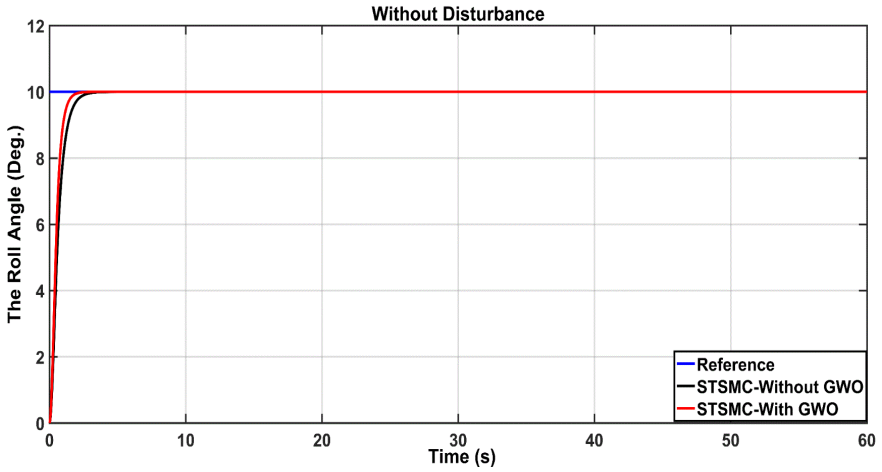

Fig. 7. Behavior of roll angle STSMC.

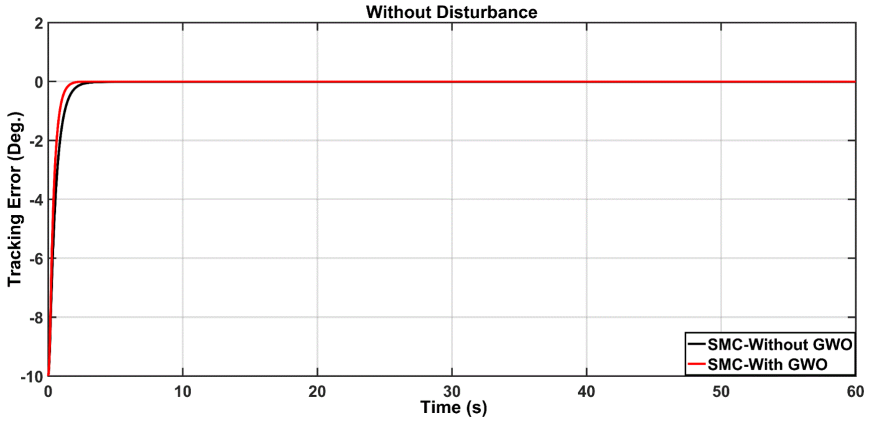

Fig. 8. Behavior of tracking errors with SMC.

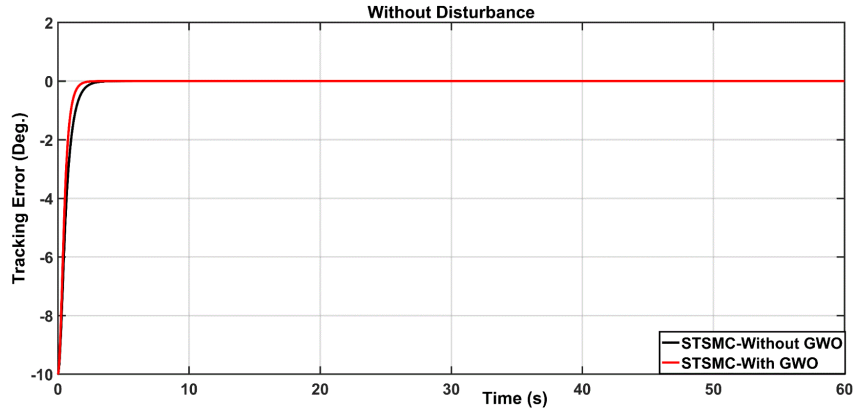

Fig. 9. Behavior of tracking errors with STSMC.

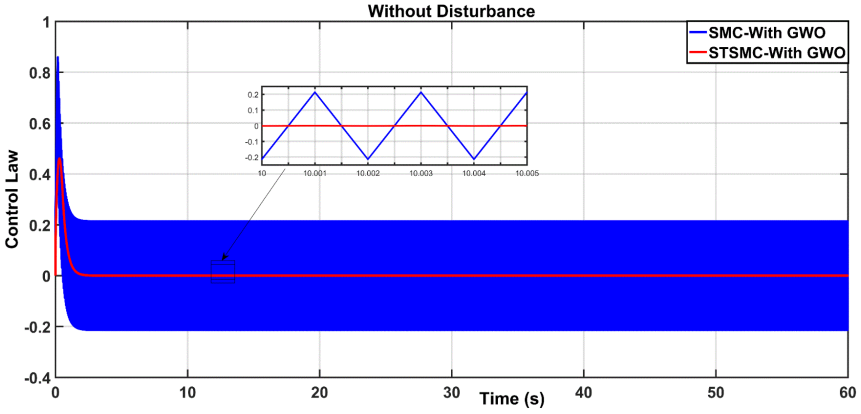

Fig. 10. The control response with uncertainty-free case.

In the next scenario, it is assumed that the aircraft is subjected to rotational gust behaviour, which represents a nonparametric uncertainty. The rotational gust component $\xi(t)$ was modeled as a sin-function of amplitude 0.1 and frequency 30 Hz. The behaviours of aircraft roll angle under gust uncertainty for both optimal

SMC and optimal STSMC are in Fig. 11. The responses of tracking errors are shown in Fig. 12. The STSMC gives less variance in error as compared to the classical SMC. The behaviour of control law resulting from this situation is illustrated in Fig. 13. Again, the STSMC could successfully eliminate the chattering level as compared to the SMC.

Table. 3 Tracking performance of tail-sitter VTOL aircraft based on the controllers.

Controller	RMSE	t_s(s)
SMC-Without GWO	0.0128	3.36
SMC-With GWO	0.0131	2.04
STSMC-Without GWO	0.0148	3.13
STSMC-With GWO	0.0113	2.19

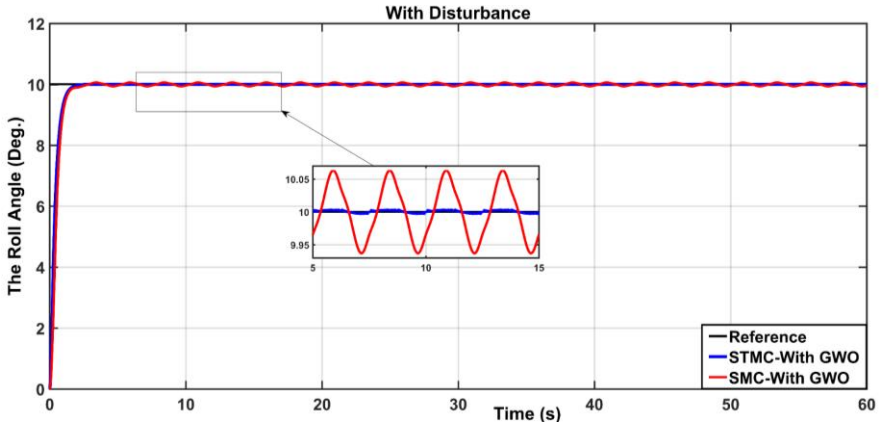

Fig. 11. Behavior of roll angle with gust wind uncertainty.

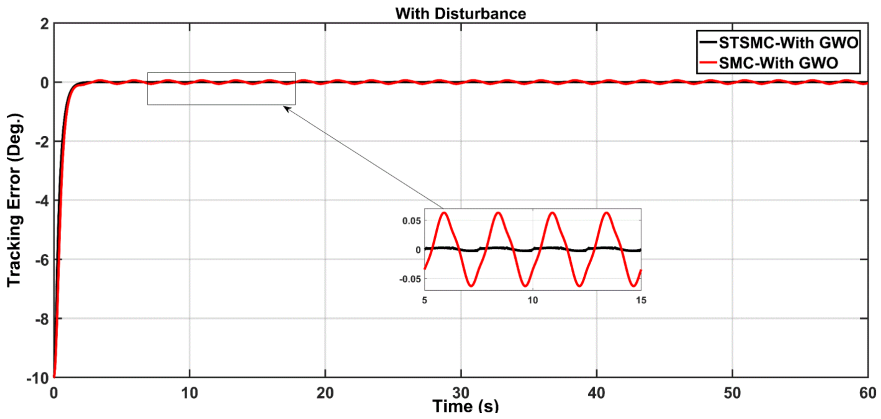

Fig. 12. Behavior of tracking errors with gust wind uncertainty.

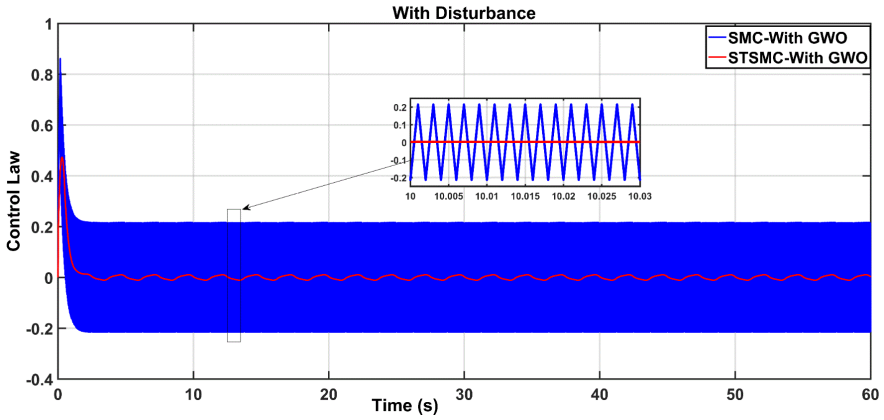

Fig. 13. The control response with gust wind uncertainty.

7. Conclusion

In this study, two schemes of sliding mode controllers are presented, STSMC and SMC, to stabilize and control the roll motion of tail-sitter VTOL aircraft. The stability of controlled aircraft system has been analysis and proved based on Lyapunov theorem. Accordingly, the control law has been established. The GWO is invoked to find the optimal setting of design parameters for both SMC and STSMC and accordingly to further improve the dynamic performance of controlled systems. A comparison study in terms of steady-state error and chattering level in control signal has been conducted for uncertainty-free case and uncertainty case. The computer simulation showed that the GWO could enhance the performances of proposed controllers. Moreover, the optimal STSMC has better performance than optimal SMC in terms of tracking error and chattering behaviour. This study will be extended in the future work to consider more degree of freedom in dynamic model of aircraft, and also taking into account the motion in three-dimensional space. One can suggest other optimization techniques like PSO, SSO, or WOA to conduct a comparison in performance with GWO in terms of minimum tracking error and computation effort indices.

Nomenclatures

c_1, k_1, k_2	Design parameters of SMC
c_2, k_3, k_4	Design parameters of STSMC
C_L	The roll damping coefficient
d	The rotor distance from the mass centre
J_x	Moment inertia in the x-axis
T_l, T_m, T_n	Thrust moments
u	Control law
u_{eq}	Equivalent part of control law
u_{sw}	Switching part of control law
$V(.)$	Lypunov function

Greek Symbols

γ	is a positive constant and it represents the upper bound of the derivative of the uncertainty
$\zeta(t)$	The gust wind

θ_d	Desired angular position
s_θ	Sliding Surface
k, λ_1	Design parameters of SMC.
c_1, c_2, λ	The design parameters of STSMC.
φ	The disturbances

Abbreviations

GWO	Grey-Wolf Optimization
HIL	Hardware-In-Loop
INDI	Incremental Nonlinear Dynamic Inversion
MPC	Model Predictive Controller
PID	Proportional Integral Derivative
PSO	Particle Swarm Optimization
SIL	Software-In-Loop
SMC	Sliding Mode Control
SSO	Spider Social Optimization
STSMC	Super Twisting Sliding Mode Control
UAV	Unmanned Air Vehicle
VTOL	Vertical Take-off Landing

References

1. Saeeda, A.S.; Younesb, A.B.; Cai, C.; and Cai, G. (2018). A survey of hybrid unmanned aerial vehicles. *Progress in Aerospace Sciences*, 98, 98-105.
2. Guerrero, J.A.; and Lozano, R. (2012). *Flight formation control*. John Wiley & Sons.
3. Barth, J.M.; Condomines, J.-P.; Bronz, M.; Moschetta, J.-M.; Join, C.; and Fliess , M. (2020). Model-free control algorithms for micro air vehicles with transitioning flight capabilities. *International Journal of Micro Air Vehicles*, 12, 1-22.
4. Zhou, W.; Li, B.; Sun, J.; Wen, C.-Y.; and Chen, C.-K. (2019). Position control of a tail-sitter UAV using successive linearization based model predictive control. *Control Engineering Practice*, 91.
5. Wang, W.; Zhu, J.; Kuang, M.; Yuan, X.; Tang, Y.; Lai, Y.; Chen, L.; and Yang, Y. (2019). Design and hovering control of a twin rotor tail-sitter UAV. *Science China Information Sciences*, 62(9).
6. Garcia-Nieto, S.; Velasco-Carrau, J.; Paredes-Valles, F.; Salcedo, J.V.; and Simarro, R. (2019). Motion equations and attitude control in the vertical flight of a VTOL bi-rotor UAV. *Electronics*, 8(2).
7. Ge, Z.; and Hou, J. (2019). Design of the control law of longitudinal attitude for tail-sitter UAV. *Proceedings of the International Conference on Applied Physics and Mathematics*. Chulalongkorn University, Thailand.
8. Abrougui, H.; Nejim, S.; and Dallagi, H. (2019). Roll control of a tail-sitter VTOL UAV. *International Journal of Control, Energy and Electrical Engineering*, 7, 22-27.
9. Flores, A.; Oca, A.M.; and Flores, G. (2018). A simple controller for the transition maneuver of a tail-sitter drone. *Proceedings of the IEEE Conference on Decision and Control*. Miami Beach, USA, 4277-4281.

10. Garcia, O.; Sanchez, A.; Escareño, J.; and Lozano, R. (2008). Tail-sitter UAV having one tilting rotor: modeling, control and real-time experiments. *Proceedings of the 17th World Congress, International Federation of Automatic Control*. Seoul, Korea, 809-814.
11. Verling, S.; Weibel, B.; Boosfeld, M.; Alexis, K.; Burri, M.; and Siegwart, R. (2016). Full attitude control of a VTOL tail-sitter UAV. *Proceedings of the 2016 IEEE International Conference on Robotics and Automation*. Stockholm, Sweden, 16-21.
12. Li, B.; Zhou, W.; Sun, J.; Wen, C.-Y.; and Chen, C.-K. (2018). Development of model predictive controller for a tail-sitter VTOL UAV in hover flight. *Sensors*, 18(9).
13. Çakici, F.; and Leblebicioğlu, M.K. (2016). Control system design of a vertical take-off and landing fixed-wing UAV. *IFAC-PapersOnLine*, 49(3), 267-272.
14. Utkin, V.; Guldner, J.; and Shi, J. (2009). *Sliding mode control in electro-mechanical systems* (2nd ed.). Florida: CRC Press.
15. Humaidi, A.J.; and Hasan, A.F. (2019). Particle swarm optimization–based adaptive super-twisting sliding mode control design for 2-degree-of-freedom helicopter. *Measurement and Control*, 52(9-10), 1403-1419.
16. Humaidi, A.J.; and Hameed, A.H. (2018). PMLSM position control based on continuous projection adaptive sliding mode controller. *Systems Science and Control Engineering*, 6(3), 242-252.
17. Feng, Z.; and Fei, J. (2018). Design and analysis of adaptive super-twisting sliding mode control for a microgyroscope. *PLoS ONE*, 13(1), 1-18.
18. Falah, A.; Humaidi, A.J.; Al-Dujaili, A.; and Ibraheem, I.K. (2021). Robust super-twisting sliding control of PAM-actuated manipulator based on perturbation observer. *Cogent Engineering*, 7(1), 1-30.
19. Al-Dujaili, A.Q.; Falah, A.; Humaidi, A.J.; Pereira, D.A.; and Ibraheem, I.K. (2020). Optimal super-twisting sliding mode control design of robot manipulator: design and comparison study. *International Journal of Advanced Robotic Systems*, 17(6), 1-17.
20. Hameed, A.H.; Al-Dujaili, A.Q.; Humaidi, A.J.; and Hussein, H.A. (2019). Design of terminal sliding position control for electronic throttle valve system: a performance comparative study. *International Review of Automatic Control*, 12(5), 251-260.
21. Mirjalili, S.; Mirjalili, S.M.; and Lewis, A. (2014). Grey wolf optimizer. *Advances in Engineering Software*, 69, 46-61.
22. Gao, Z.-M.; and Zhao, J. (2019). An improved grey wolf optimization algorithm with variable weights. *Computational Intelligence and Neuroscience*, 2019, 1-13.
23. Uddin, M.N.; Amin, I.K.; Rezaei, N.; and Marsadek M. (2018). Grey wolf optimization based power management strategy for battery storage of DFIG-WECS in standalone operating mode. 2018 *IEEE Industry Applications Society Annual Meeting* (*IAS*), 1-7,
24. Wong, K.C.; Guerrero, J.A.; Lara, D.; and Lozano, R. (2007). Attitude stabilization in hover flight of a mini tail-sitter UAV with variable pitch propeller. *Proceedings of the IEEE/RSJ International Conference on Intelligent Robots and Systems*. San Diego, USA, 2642-2647.

25. Stevens, B.L.; Lewis, F.L.; and Johnson, E.N. (2016). *Aircraft control and simulation: dynamics, controls design, and autonomous systems* (3rd ed.) New Jersey: John Wiley & Sons, Inc.
26. Humaidi, A.; and Hameed, M. (2019). Development of a new adaptive backstepping control design for a non-strict and under-actuated system based on a PSO tuner. *Information*, 10(2), 1-17.
27. Sherwani, K.I.K.; Kumar, N.; Chemori, A.; Khan, M.; and Mohammed, S. (2020). RISE-based adaptive control for EICoSI exoskeleton to assist knee joint mobility. *Robotics and Autonomous Systems*, 124, 1-28.
28. Humaidi, A.J.; Badr, H.M.; and Hameed, A.H. (2018). PSO-based active disturbance rejection control for position control of magnetic levitation system. *Proceedings of the 5th International Conference on Control, Decision, and Information Technologies*. Thessaloniki, Greece, 922-928.
29. Belherazem, A.; and Chenafa, M. (2021). Passivity based adaptive control of a single-link flexible manipulator. *Automatic Control and Computer Sciences*, 55, 1-14.
30. Humaidi, A.J.; Kadhim, S.K.; and Gataa, A.S. (2020). Development of a novel optimal backstepping control algorithm of magnetic impeller-bearing system for artificial heart ventricle pump. *Cybernetics and Systems: An International Journal*, 51(4), 521-541.
31. Dewasme, L.; and Wouwer, A.V. (2020). Model-free extremum seeking control of bioprocesses: a review with a worked example. *Processes*, 8(10).
32. Humaidi, A.J.; Ibraheem, I.K.; Azar, A.T.; and Sadiq, M.E. (2020). A new adaptive synergetic control design for single link robot arm actuated by pneumatic muscles. *Entropy*, 22(7), 1-24.
33. Humaidi, A.J.; Badr, H.M.; and Ajil, A.R. (2018). Design of active disturbance rejection control for single-link flexible joint robot manipulator. *Proceedings of the 22nd International Conference on System Theory, Control and Computing*. Sinaia, Romania, 452-458.
34. Nayl, T.; Nikolakopoulos, G.; and Gustafsson, T. (2015). Effect of kinematic parameters on MPC based on-line motion planning for an articulated vehicle. *Robotics and Autonomous Systems*, 70, 16-24.
35. Humaidi, A.J.; Oglah, A.A.; Abbas, S.J.; and Ibraheem, I.K. (2019). Optimal augmented linear and nonlinear PD control design for parallel robot based on PSO tuner. *International Review on Modelling and Simulations*, 12(5). 281-291.
36. Humaidi, A.J.; and Abdulkareem, A.I. (2019). Design of augmented nonlinear PD controller of Delta/Par4-like robot. *Journal of Control Science and Engineering*, 2019, 1-11.
37. Humaidi, A.J.; Hameed, M.R.; and Hameed, A.H. (2018). Design of block-backstepping controller to ball and arc system based on zero dynamic theory. *Journal of Engineering Science and Technology*, 13(7), 2084-2105.
38. Saleh, M.H.; Al-Qassar, A.; Othman, M.Z.; and Mahdi, A.S. (2010). Development of the cross-coupling phenomena of MIMO flight system using fuzzy logic controller. *Journal of Engineering Science and Technology* (*JESTEC*), 5(1), 85-93.
39. Al-Qassar, A.A.; Al-Dujaili, A.Q.; Hasan, A.F.; Humaidi, A.J.; Ibraheem, I.K.; and Azar, A.T. (2021). Stabilization of single-axis propeller-powered system

for aircraft applications based on optimal adaptive control design. *Journal of Engineering Science and Technology* (*JESTEC*), 16(3), 1851-1869.

40. Nayl, T.; Nikolakopoulos, G.; Gustafsson, T.; Kominiak, D.; and Nyberg, R. (2018). Design and experimental evaluation of a novel sliding mode controller for an articulated vehicle. *Robotics and Autonomous Systems*, 103, 213-221.
41. Nadimi-Shahraki, M.H.; Taghian, S.; and Mirjalili, S. (2021). An improved grey wolf optimizer for solving engineering problems. *Expert Systems with Applications*, 166.
42. Hu, P.; Pan, J.-S.; Chu, S.-C. (2020). Improved binary grey wolf optimizer and its application for feature selection. *Knowledge-Based Systems*, 195.
43. Yue, Z.; Zhang, S.; and Xiao, W. (2020). A novel hybrid algorithm based on grey wolf optimizer and fireworks algorithm. *Sensors*, 20(7).
44. Yetkin, M.; and Bilginer, O. (2020). On the application of nature-inspired grey wolf optimizer algorithm in geodesy. *Journal of Geodetic Science*, 10, 48-52.
45. Geleta, D.K.; Manshahia, M.S.; Vasant, P.; and Banik, A. (2020). Grey wolf optimizer for optimal sizing of hybrid wind and solar renewable energy system. *Computational Intelligence*, 1-30.
46. Humaidi, A.J.; Najem, H.T.; Al-Dujaili, A.Q.; Pereira, D.A.; Ibraheem, I.K.; Azar, A.T. (2021). Social spider optimization algorithm for tuning parameters in PD-like interval type-2 fuzzy logic controller applied to a parallel robot. *Measurement and Control*, 54(3-4), 1-21.
47. Al-Azza, A.A.; Al-Jodah, A.A.; and Harackiewicz, F.J. (2015). Spider monkey optimization: a novel technique for antenna optimization. *IEEE Antennas and Wireless Propagation Letters*, 15, 1016-1019.
48. Moezi, S.A.; Zakeri, E.; and Zare, A. (2018). A generally modified cuckoo optimization algorithm for crack detection in cantilever Euler-Bernoulli beams. *Precision Engineering*, 52, 227-241.
49. Mirjalili, S. (2016). SCA: a sine cosine algorithm for solving optimization problems. *Knowledge-Based Systems*, 96, 120-133.
50. Allawi, Z.T.; Ibraheem, I.K.; and Humaidi, A.J. (2019). Fine-tuning meta-heuristic algorithm for global optimization. *Processes*, 7(10), 1-14.
51. Nasiri, J.; and Khiyabani, F.M. (2018). A whale optimization algorithm (WOA) approach for clustering. *Cogent Mathematics & Statistics*, 5(1), 1-13.